Implementation and validation of nonlinear elastic models to simulate soil behavior

Ana Rita Parente Mariquitos

Master in Civil Engineering

Instituto Superior Técnico, Universidade de Lisboa, Portugal

Email: ana.rita.mariquitos@tecnico.ulisboa.pt

Abstract - In the last decades the practice of geotechnical engineering has evolved in a way that it is now possible to model and analyze complex structures as well as soil / structure interaction problems through numerical modeling (for instance: using the finite element method or finite differences).

Numerical methods are a tool with great potential, but the validity of the results obtained by their application depends on the constitutive models adopted to describe the behavior of the geomaterials.

This dissertation summarizes the various elements necessary for the formulation of constitutive models used to reproduce soil behavior, and implements constitutive equations in an incremental format for two non-linear elastic models: K-G model and Jardine model (also known as small strain stiffness model), in the commercial software, PLAXIS. The validation of these models is done through the simulation of laboratory tests. In addition, two algorithms for stress integration – Euler and Modified Euler, with and without substepping - were implemented and compared.

Key words: *Small Strain Stiffness Model,* K-G Model, Finite Element Method, Stress Integration Algorithms

1. Introduction

The number of users that use software based on the finite element method has increased dramatically in the last 15 years, especially among young professionals. This is mainly due to the large-scale commercialization of specialized software coupled with the rapid technological evolution and the need to build, for example, in urban areas where the analysis of the interaction between the structure to be dimensioned and the adjacent ones is more relevant. This dissertation aims to analyze the potentialities and limitations of some constitutive models used to reproduce soil behavior, as well as to present in a generalized way the various elements necessary for the formulation of different types of constitutive models (linear and nonlinear elastic, elastic perfectly plastic and elastoplastic).

2. Newton-Raphson Method

There are several strategies for dealing with nonlinear elastic and / or elastoplastic problems. All involve writing Equation (1) in global incremental form:

$$[K_G]^i\{\Delta v_G\}^i = \{\Delta F_G\}^i \tag{1}$$

Where $[K_G]^i$ is the incremental global stiffness matrix, $\{\Delta v_G\}^i$ is the vector of incremental nodal displacements, $\{\Delta F_G\}^i$ is the vector of incremental nodal forces and finally, i is the increment number. Thus for each increment, equation (2) must be solved, and the final solution of $\{\Delta v_G\}$ is obtained by summing the results $\{\Delta v_G\}^i$ for all increments. However, due to the nonlinear constitutive behavior, $[K_G]^i$ depends on the current stress and / or strain, not being constant, that is, it varies over an increment.

The Newton-Raphson method evaluates the behavior of the soil within or very close to a possible stress space. Thus, recalling equation (2) applied to this problem:

$$[K_G]^i\{\Delta v\}^i = \{F_{ex}\}^i - \{F_{in}\}^{i-1} \tag{2}$$

Where $[K_G]^i$ is the global tangent stiffness matrix of increment *i*, $\{\Delta v\}^i$ is the vector of incremental displacements associated with increment *i*, $\{F_{ex}\}^i$is the applied external load vector, $\{F_{in}\}^{i-1}$ is the internal force vector of the previous increment and *i* refers to the increment number. It is then possible to divide an increment into several iterations:

$$[K_G]^j\{\delta v\}^j = \{F_{ex}\}^i - \{F_{in}\}^{j-1} \tag{3}$$

Where, j refers to the number of the iteration, δv is a vector containing iterated displacements, which contribute to the increments of displacements of the increment i:

$$\{\Delta v\}^i = \sum_{j=1}^{n} \{\delta v\}^j \tag{4}$$

In addition, $\{F_{in}\}$ is calculated using the following formula, where, $\{\sigma_c^{i-1}\}$ refers to the vector of constitutive stresses and $[B]$ is the strain interpolation matrix. The integration of tensions will be addressed in the next section.

$$\{F_{in}\} = \int [B]^T\{\sigma_c^{i-1}\}dV \tag{5}$$

2.1. Stress point algorithms

- **Euler Method with substepping (ME)**

It is the most basic first-order explicit method (Atkinson, 1989), which means that the local error (that is, the error per step) is proportional to the square of the step size, and the overall error is proportional to the size of the step. Adapting this method to the present theme:

$$\{\sigma\}^{i+1} = \{\sigma\}^i + [D] \times (\{\varepsilon\}^{i+1} - \{\varepsilon\}^i) \tag{6}$$

Where $[D]$ is the tangent stiffness matrix of the material for state *i* and $\{\varepsilon\}^i$ is the vector of strain increments in the same substep. In this method a very small value of $\{\varepsilon\}^{i+1} - \{\varepsilon\}^i$ is required to obtain approximate values, however this implies increasing the number of substeps performed, also increasing the calculation time.

For the substepping, this integration algorithm considers a counter (n) that determines the number of subdivisions in which the deformation increment is to be divided.

- **Modified Euler Method with substepping (MME)**

One of the causes for increasing errors in the Euler method is that $[D]$, at the initial point $(\varepsilon_i, \sigma_i)$, is applied to the total interval. In order to reduce the error arising from this cause, there are modifications that can be performed, such as the modified Euler method, also known as the midpoint method. Briefly, this method calculates the function $[D]$ at the midpoint $(\varepsilon_{i+1/2}, \sigma_{i+1/2})$ of the interval $(\varepsilon_i, \sigma_i)$ and then obtains $\{\sigma\}^{i+1}$ in a similar way to Euler Method (6). The substepping is also implemented in a similar manner to Euler's algorithm.

3. K-G Model

This nonlinear elastic model proposed by Naylor et al. (1981) considers that the bulk modulus K and shear modulus G are tangent and explicitly defined in terms of stress invariants, mean effective stress, p' and deviatoric stress, q, or alternatively as a function of the quantities σ_{mean} and σ_{dev}. When the Mohr-Coulomb failure criterion is to be incorporated, it is convenient to express the modules K and G in function of these invariants defined by the following equations:

$$\sigma_{mean} = \frac{\sigma_1 + \sigma_3}{2} \quad ; \quad \sigma_{dev} = \sigma_1 - \sigma_3 \tag{7) (8}$$

$$K_t = K_i + \alpha_K . \sigma_{mean} \tag{9}$$

$$G_t = G_i + \alpha_G . \sigma_{mean} + \beta_G . \sigma_{dev} \tag{10}$$

In this way, K and G grow with increasing σ_{mean} and G decreases with σ_{dev}, tending to zero at failure, and therefore at failure the Poisson ratio tends to 0.5. It is recommended to set a maximum value for the Poisson ratio of 0.495. It was verified that in numerical analyzes with values of Poisson ratio close to 0,49999, it is not possible to invert the stiffness matrix due to numerical instability (for example, the pivot matrix element is negative during the inversion process), (Potts & Zdravkovic, 1999).

The parameters G_i, α_G and β_G must be chosen or calculated in such a way that the failure criterion is satisfied, that is, when the acting stresses obey the failure criterion and G is zero:

$$G_i + \alpha_G . \sigma_{méd} + \beta_G . \sigma_{dev} = 0 \tag{11}$$

From the above equation it is possible to obtain the following relations:

$$\frac{\alpha_G}{-\beta_G} = 2 \sin \varphi' \quad ; \quad \frac{G_i}{-\beta_G} = 2 . c' . cos\, \varphi' \tag{12) (13}$$

Thus, instead of manually determining 5 input parameters (some of which appear to have no immediate physical significance), it is possible for known values of the angle of shearing resistance, φ', and soil cohesion, c', to obtain the values of α_G and β_G with (12) and (13), where G_i is a value fixed by the user. Therefore, it is not necessary to obtain some of the parameters through triaxial tests (K_i, α_K, G_i, α_G e β_G), however the model still requires 5 input parameters.

4. Jardine Model (Small Strain Stiffness Model)

The non-linear behavior in the range of small strains is not very often taken into account. Analyses that do not consider this behavior often end up overestimating the strains in the points of the domain subject to small perturbations (small increments of stress) and underestimating maximum strains of structures.

Thus, Jardine model, also known as Small Strain Stiffness Model, was chosen out of the several models present in the literature. This model defines soil stiffness for small strains in the range $10^{-5} - 10^{-3}$ (Jardine et al. 1986), through two logarithmic periodic functions expressing the nonlinear relationship between tangent normalized distortion modulus and shear / distortion strain, and the nonlinear relationship between normalized tangent bulk modulus and volumetric deformation. Thus the equations of the trigonometric curves are as follows:

$$\frac{3G_t}{p'} = \mathrm{A} + \mathrm{B}\cos(\alpha \mathrm{X}^{\gamma}) - \frac{\mathrm{B}\alpha\gamma \mathrm{X}^{\gamma-1}}{2.303}\sin(\alpha \mathrm{X}^{\gamma}) \tag{14}$$

$$\frac{\mathrm{K_t}}{p'} = \mathrm{R} + \mathrm{S}\cos(\delta \mathrm{Y}^{\eta}) - \frac{\mathrm{S}\delta\eta \mathrm{Y}^{\eta-1}}{2.303}\sin(\delta \mathrm{Y}^{\eta}) \tag{15}$$

With:

$$\mathrm{X} = \log_{10}\left(\frac{2\varepsilon_{dev}}{3\mathrm{C}}\right) = \log_{10}\left(\frac{2\sqrt{\frac{1}{2}[(\varepsilon_1-\varepsilon_2)^2+(\varepsilon_2-\varepsilon_3)^2+(\varepsilon_1-\varepsilon_3)^2]}}{3\mathrm{C}}\right) \tag{16}$$

$$\mathrm{Y} = \log_{10}\left(\frac{\varepsilon_{\mathrm{vol}}}{\mathrm{T}}\right) = \log_{10}\left(\frac{\varepsilon_1+\varepsilon_2+\varepsilon_3}{\mathrm{T}}\right) \tag{17}$$

Where K_t is the bulk stiffness modulus, G_t is the shear modulus, p' 'is the mean effective stress, ε_i are the principal strains, and A, B, C, R, S, T, α , γ, δ and η are empirical constants. There are also the limits $\varepsilon_{volmax} > \varepsilon_{vol} > \varepsilon_{volmin}$ and $\varepsilon_{dmax} > \varepsilon_{dev} > \varepsilon_{dmin}$. This model was copled with a plastic model with a Mohr-Coulomb criterion that has three input parameters (shear resistance angle, φ', dilation angle, ψ, and soil cohesion, c').

5. Model Validation with Conventional Triaxial Tests

5.1. K-G Model

Consolidated drained triaxial tests (CD) with different confining pressures of 100 kPa, 200 kPa and 300 kPa were modelled in PLAXIS using the Euler Method and the Modified Euler Method for different values of n (1, 5, 10 and 20). In addition, consolidated undrained triaxial tests (CU) were simulated with the same confining pressures with the two integration methods for n equal to 1 and 10. Table 1 presents the input parameters used in PLAXIS.

Table 1: K-G Model parameters

Parameters	Name	Units	Value
1	K_i	kPa	10000
2	G_i	kPa	100

3	α_K	-	100
4	φ'	degree	30
5	cohesion	kPa	1

- **Consolidated drained triaxial tests (CD)**

In Figure 2 it is possible to observe the modeling results for the two algorithms discussed above using the same number of cycles. In general, it is verified that the MMME algorithm obtains adequate results using a smaller number of *n* than the algorithm ME in the same conditions.

For the shear phase it is necessary to consider how both algorithms behave for abrupt variations in the soil stiffness matrix during the simulation. For example, when considering a unit number of *n* for the Euler Method, although there is subincrementation and an expedient method, the results are not satisfactory. Thus, the results of these simulations, which correspond to ME: n = 1, are not satisfactory since the obtained curves have difficulty in adjusting to that of the approximate solution (from shear strains higher than 1,7% - Fig: 2 b)).

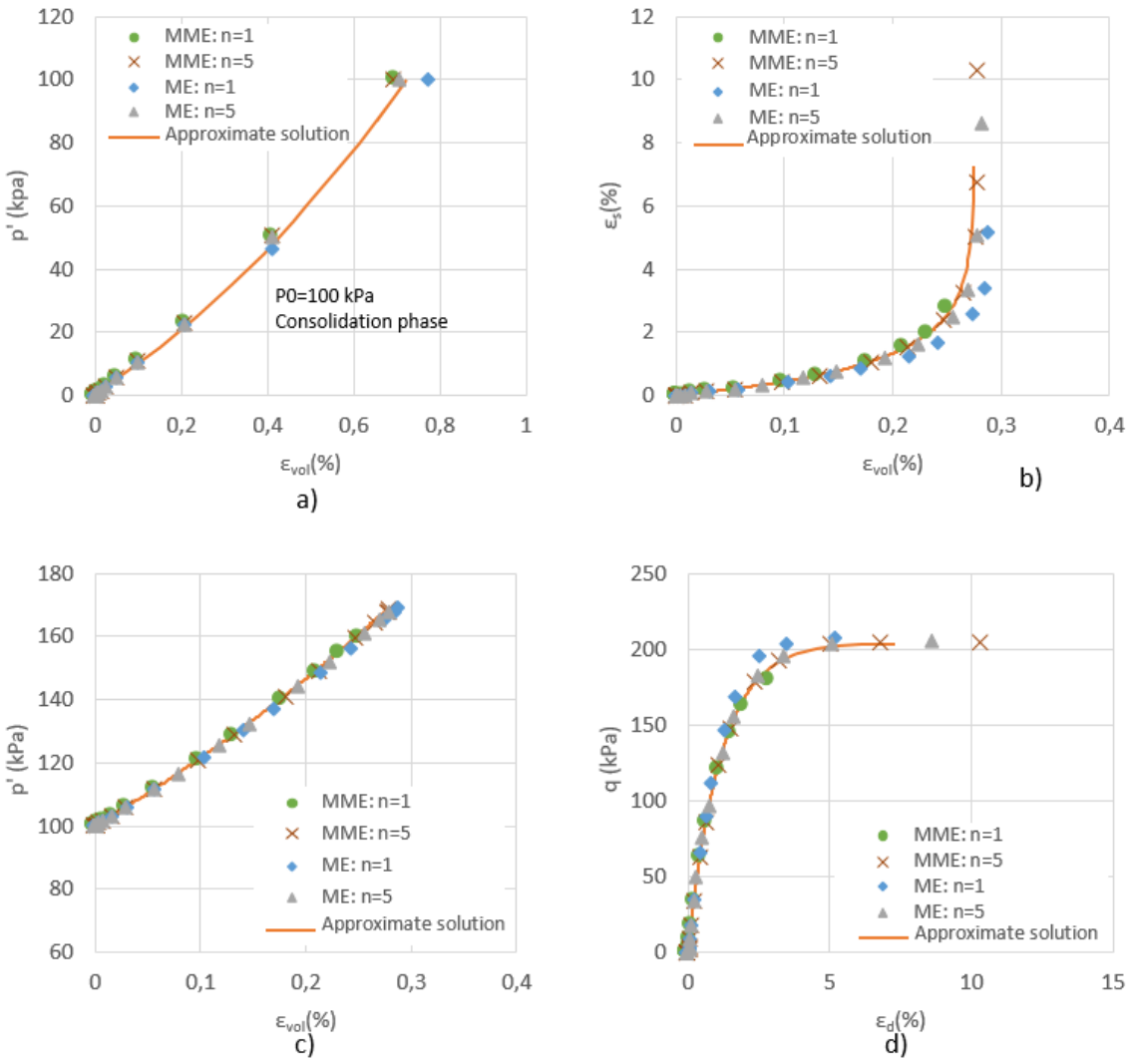

Fig. 1: Drained triaxial tests with confining stress 100 kPa for different algorithms with equal n

In addition, it is possible to affirm that MME algorithm allows closer results to the solution for a smaller value of *n*, however from a certain number of n, it is not possible to refine the results (n = 5). This is not true for ME where it is possible to improve the response up to n = 10.

- **Consolidated undrained triaxial tests (CU)**

The consolidation phase of these tests is similar to the drained triaxial tests so it will not be addressed.The Modified Euler Method algorithm with n = 1 presents satisfactory results when compared with Euler Method's algorithm for the same number of cycles and the solution. In fact, the points corresponding to the Euler Method algorithm for the same number of cycles (n = 1), deviate from the other results, exceeding 10 kPa of the mean value of the curves (Fig: 3 a)), being unreasonable.

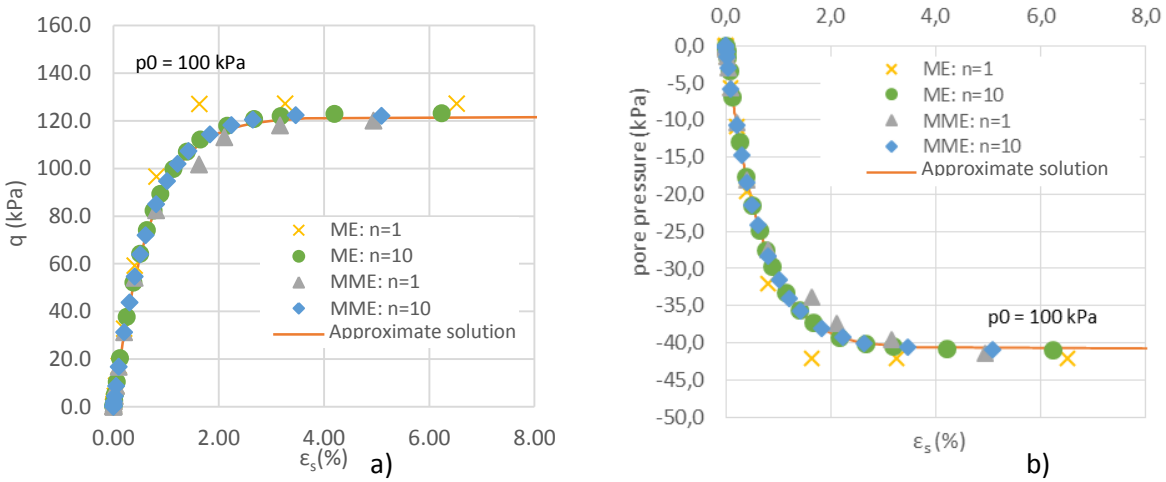

Fig. 2 Undrained triaxial tests with confining stress 100 kPa for different algorithms with equal *n*

For n = 10, both algorithms present satisfactory results, with well delimited curves with enough points in areas of abrupt tangent variation. Note also that for an intermediate value of *n*, not shown here, the MME algorithm converges very quickly to a solution than the ME algorithm.

5.2. Jardine Model

Drained triaxial tests were performed with Jardine model with failure criterion for different confining stresses (100, 200 and 300 kPa). The dilation angle (ψ) was defined at 0 °, 15 ° and 30 °, and the value of the shearing resistance angle (ϕ) was set at 30 °. The Euler Modified Method algorithm was used with n = 10. Additionally, it was possible to measure an approximate solution of the Jardine model using the equations (14) and (15) as a function of the normalized shear and volumetric moduli and respective strains. Similarly, undrained triaxial tests for different confining stresses (100, 200 and 300 kPa) were performed in the PLAXIS. The parameters used are listed in Table 2.

Table 2: Jardine model input parameters

Props	**1**	**2**	**3**	**4**	**5**	**6**	**7**	**8**	**9**	**10**
Parameter	A	B	C	R	S	T	α	γ	δ	η
Units	-	-	%	-	-	-	-	-	-	-
Props	**11**	**12**	**13**	**14**	**15**	**16**	**17**	**18**	**19**	**20**
Parameter	Evmax	Evmin	Edmax	Edmin	Gnorm	Knorm	ncyle	ϕ	ψ	cohesion
Units	%	%	%	%	kPa	kPa	-	(°)	(°)	kPa

The points obtained through numerical modeling coincide with those of the approximate solution in general. The sharp degradation of the stiffness (normalized by the effective mean stress, p ') with the occurrence of strains is clearly observed.

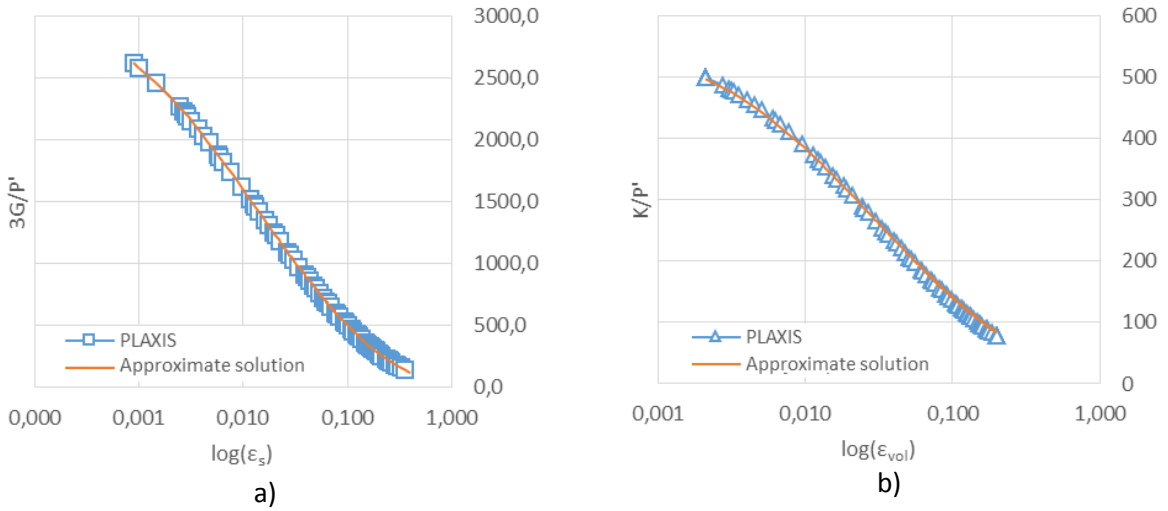

Fig. 3 Comparison of the variation of the volumetric and normalized shear moduli between numerical modeling and approximate solution of the Jardine model

- **Consolidated drained triaxial tests (CD)**

In Fig. 5 a) the trajectories of the total and effective stresses are presented for confining stresses of 100, 200 and 300 kPa as well as the envelope of allowable stresses for the Mohr-Coulomb failure criterion. The stresses trajectories slightly exceed the Mohr-Coulomb permissible stresses envelope. For example, the theoretical failure stress at a confining stress of 100 kPa is 303.46 kPa and the failure stress obtained through the modeling was 304.61 kPa, which means there is an error of 0.37%. In Fig. 5 b), the behavior of this model in relation to the variation of the angle of dilation (0 °, 15 ° and 30°), where $\psi < \varphi'$ results in non-associated conditions (i.e., non-associated flow rate law).

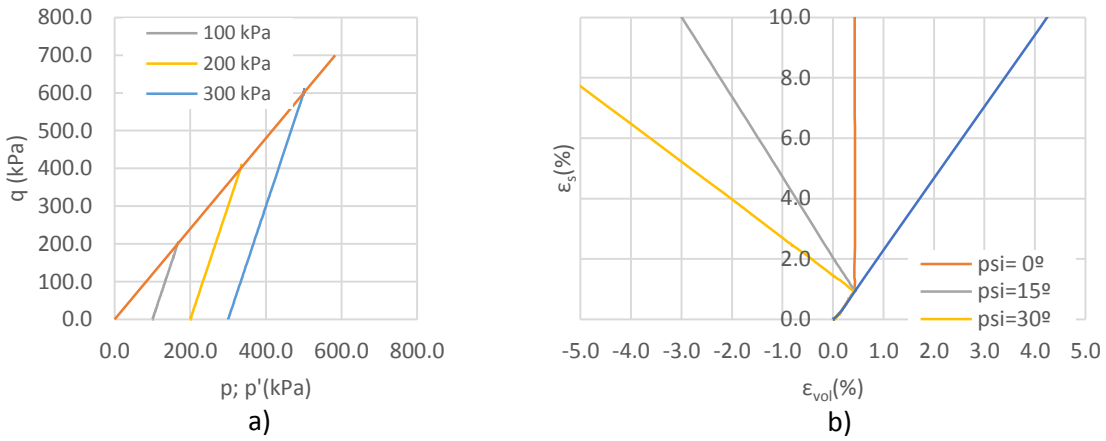

Fig. 4 a) Stress trajectories for confining stresses of 100, 200 and 300 kPa (Jardine Model with Mohr-Coulomb Failure Criterion b) Relation between volumetric strains and deviatorical strains in the shear phase for p0 = 100 kPa (CD)

It was found that regardless of the value adopted for the dilatation after failure, stresses in the soil element remain constant. In terms of strain, for angles of dilation greater than 0 °, it is verified that after reaching the failure the volumetric strain begins to decrease (ie, the soil dilates). If an angle of dilation of 0 ° is allowed, there is no plastic dilatation and no plastic volumetric strain occurs (Fig: 6).

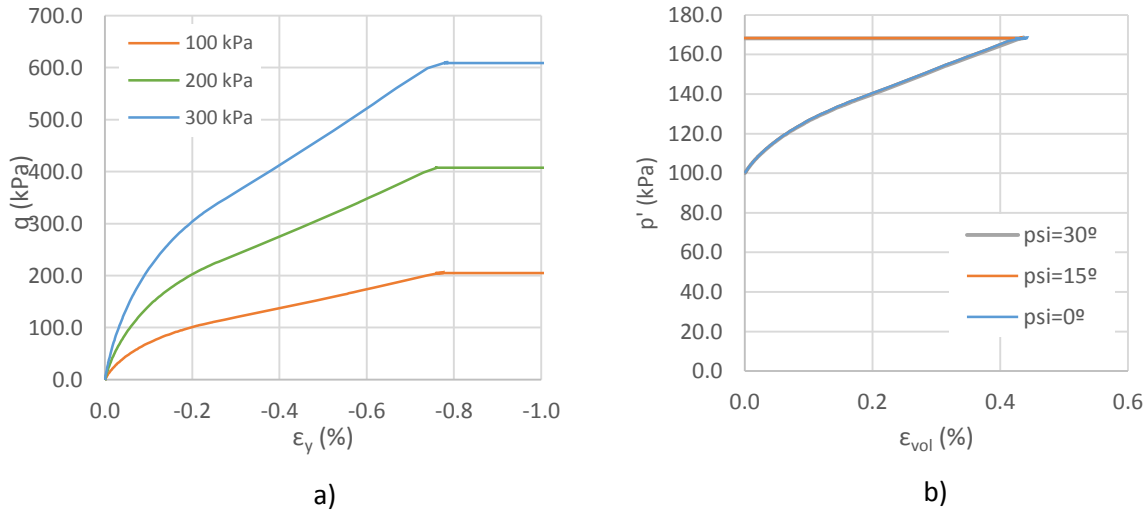

Fig. 5 Results of the triaxial tests drained for p0 = 100, 200 and 300 kPa of the Jardine Model with Mohr-Coulomb Failure Criterion (CD)

- **Consolidated undrained triaxial tests (CU)**

The trajectories of the effective and total stress at a confining stress of 100 kPa with 0 ° and 15 ° dilation angles are shown in Fig. 7 (a) and (b). The trajectory where an angle of dilation of 30 ° is defined is not shown since it is similar to that of 15 °.

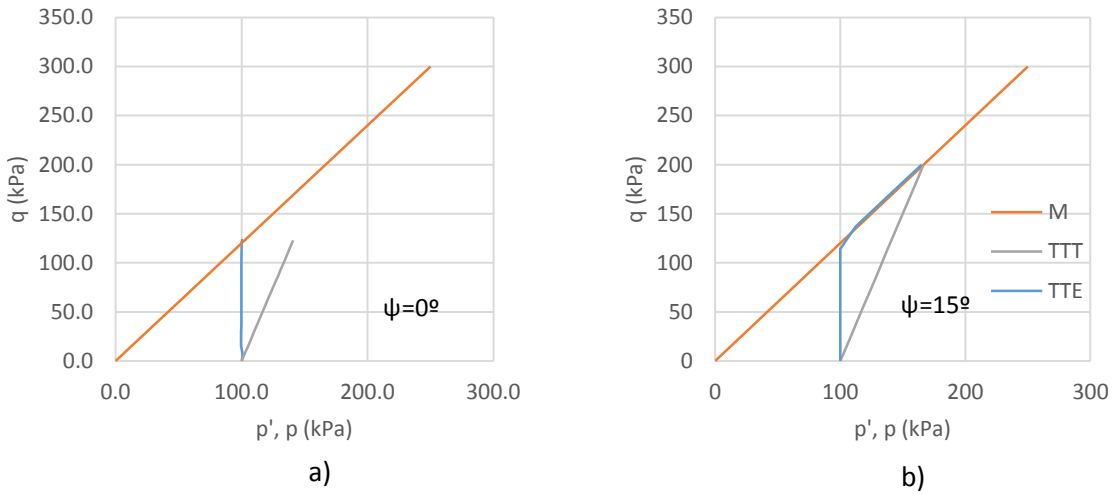

Fig. 6 a) Stress trajectories for confining stresses of 100, 200 and 300 kPa with ψ=0º and b) ψ=15º

It is known that soil tends to dilate during the drained shearing phase and also exhibits a tendency to decrease the pore pressure during the undrained shearing phase, which results in an increase in the effective stresses. Similarly, a soil that tends to compress during shearing under drained conditions exhibits an increase in excess pore pressures during shearing under undrained conditions, resulting in a decrease in effective stress. This constitutive model is able to model this behavior when failure is reached, where the input parameter, **ψ**, governs the dilation of the soil model (Fig. 8 a) and b)).

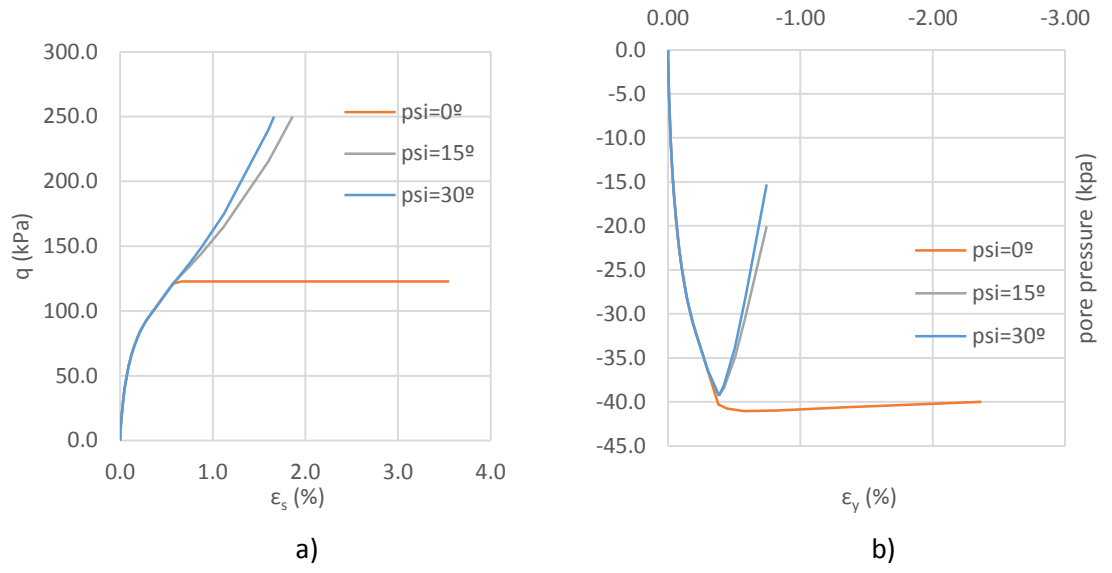

Fig. 7 a) Relation between deviatoric strain and stress b) Relation between pore pressure and vertical strain (UD)

The Jardine model fails to model real soil behavior in that it usually dilates initially near failure but for large strains reaches a constant volume condition.

6. Conclusions

It is possible to affirm that the numerical modeling and validation of the constitutive models of the soil as well as the coupling with a criterion of rupture was performed with satisfactory results for PLAXIS v8.2.

For the K-G model, it was not possible to truly couple a plastic model (Mohr-Coulomb Model), due to its formulation incorporating a Mohr-Coulomb failure criterion when *G* is equal to or close to zero. This constitutive model presents as a limitation the fact that it cannot incorporate negative / positive dilation of the soil, since it is an elastic model. In this way, there is only variation of ε_{vol} if there is mean stress variation, underestimating the volumetric compressive strain. In order to validate the model, the triaxial tests were drained and non-drained for different confining stresses with satisfactory results.

The Jardine model presents a highly nonlinear elastic behavior in the spectrum of small strains (1%) as expected. From this value, constant values are assumed for the relations $\frac{3G_t}{p'}$ e $\frac{K_t}{p'}$ and the stiffness only changes with mean stress. For the various tests carried out with different confining stresses, it was found that the stiffness parameters depend on the applied confining stresses (as in a real soil test). Obtaining the input parameters is expedient, despite the amount required, however, highly specialized laboratory equipment with limited availability is required.It was also possible to successfully couple a plastic model with Mohr-Coulomb failure criterion. Contrary to what happened for the K-G model, it was possible to vary the angle of dilation (0 °, 15 ° and 30 °), setting the angle of shearing resistance to 30 °. Thus it was possible to simulate situations with associated and non-associated flow rule in drained and undrained conditions, with results identical to those expected theoretically. A limitation of the Mohr-Coulomb plastic model is that even with non-associated conditions, where it is possible to define the ratio between volumetric and shear strains, for a non-zero dilation angle, the model predicts an increase in volumetric strains after failure through shearing. One way to circumvent this problem would be to vary the magnitude of the angle of dilation, ψ, according to the plastic shear strain,ε_d^p, as suggested by Potts (2001).

7. References

Atkinson, K. (1989). *An introduction to numerical analysis*. Wiley.

Jardine, R. J., Burland, J. B., Fourie, a. B., & Potts, D. M. (1986). Studies of the influence of non-linear stress–strain characteristics in soil–structure interaction. *Géotechnique*, *36*(3), 377–396.

Naylor, D. J., Pande, G. N., Simpson, B. and Tabb, R., (1981). Finite elements in geotechnical engineering, Pineridge Press, Swansea, U. K..

Potts, D., & Zdravkovic, L. (1999). *Finite element analysis in geotechnical engineering*. *Technology*. ThomasTelford.

Potts, D., & Zdravkovic, L. (2001). *Finite Element Analysis in Geotechnical Engineering: application*. *Zhurnal Eksperimental'noi i Teoreticheskoi Fiziki*. Thomas Telford Publishing.